Ionic liquids and ionic liquid crystals of vinyl functionalized imidazolium salts†

Shih-Ci Luo, Shaowen Sun, Amol R. Deorukhkar, Jung-Tang Lu, Amitabha Bhattacharyya and Ivan J. B. Lin*

Received 30th August 2010, Accepted 15th October 2010
DOI: 10.1039/c0jm02875d

1-Vinyl-3-alkylimidazolium salts ([C_nVIm]X, (where, C_nVIm = vinylimidazolium cation with alkyl chains of C_nH_{2n+1}; n = 4, 6, 8, 10, 12, 14, 16 and 18 for X = Br and I, and n = 12, 14, 16 and 18 for X = BF_4 and PF_6), were prepared and characterized. Ethyl substituted congeners [C_{16}EIm]Br and [C_{16}EIm]I were also prepared to understand the unique property of the vinyl substitution. Salts with shorter alkyl chain lengths ($n \leq 12$) are either room temperature or close to room temperature ionic liquids, whereas those with longer alkyl chain lengths are ionic liquid crystals with SmA mesophase. Diffractograms from powder X-ray diffraction studies suggest that in the solid state the [C_nVIm]Br series salts adopt a double bilayer structure, whereas the ethyl substituted analogues and salts in the I^-, BF_4^- and PF_6^- series have a simple bilayer structure. The thermal behavior of [C_{16}VIm]Br and [C_{16}VIm]I was compared with their saturated congeners. The vinyl functionalized salts, have slightly higher melting points and much higher clearing points than those of the saturated congeners, and therefore wider mesophases are found for the formers. Nuclear magnetic resonance spectroscopic studies suggest that vinyl functionalization provides additional hydrogen bonding interactions between the cations and anions.

Introduction

In the middle of the 1990s a renaissance of molten salts begun, which continues to flourish, in particular imidazolium based ionic liquids (ILs). This is because of their favorable properties such as thermal stability, non-flammability, high ionic conductivity, negligible vapor pressure, and a wide electrochemical window, *etc*.[1–7] Additionally, these properties can be judiciously tuned by varying the *N*-alkylimidazolium substituent and/or the anion.[8–10] These ILs are very popular and enjoy a plethora of application in various domains.[11–26] Vinylimidazolium salts were first synthesized by Salamone *et al.* as early as 1973,[27] and only after 2000 have vinylimidazolium salts received increasing attention.[28–31] Vinylimidazolium salts have served as good electrolytes in dye sensitized solar cells (DSSCs)[32,33] due to their high charge density and mobility, and also have been used in combination with lithium salts as ion conductive matrices, which provide a high ionic conductivity.[34] In addition, the presence of a vinyl moiety makes these salts polymerizable, often yielding a mechanically superior poly-electrolyte.[35–41]

Ionic liquid crystals (ILCs) are ILs exhibiting liquid crystalline properties.[42] In many imidazolium salts, ILCs can be generated simply by increasing the alkyl chain length to increase the self-organization character.[43–48] Liquid crystalline imidazolium salts possess anisotropic properties and may thus be exploited to make new materials.[49,50] Most studied imidazolium-based ILCs have been restricted to 1-alkyl-3-methylimidazolium and *N*,*N*′-dialkylimidaozlium salts.[42] Varying the substituent pattern has not been explored very much; apart from the length of the alkyl chain, a few recent examples reported the introduction of functionalized motifs such as pendant hydroxyl group on the alkyl chain,[44,51] functionalized aryl groups,[52–55] amide groups,[56,57] *etc*. Surprisingly, in spite of the many studies on vinylimidazolium salts,[58–60] only one report deals with the use of lyotropic ionic liquid crystal, 1-decyl-3-vinylimidazolium chloride, as material matrix for encapsulation of gold nanoparticles in aqueous domains and demonstrated the possibility of using this hybrid material to enhance the bulk conductivity properties.[61,62]

With these few precedents, we aimed at exploring the liquid crystal (LC) behavior of the vinylimidazolium salts. In order to study the influence of alkyl-chain length and the effect of counter anions on the LC behavior, a range of vinylimidazolium salts with different chain lengths and anions of Br^-, I^-, BF_4^-, and PF_6^- were synthesized. The effect of the vinyl substituent was studied by comparing the structures, thermal behaviors, and cation–anion interactions of the vinylimidazolium salts with the saturated congeners of ethylimidazolium salts.

Results and discussion

Vinyl imidazolium salts, denoted as [C_nVIm]X (where, C_nVIm = vinylimidazolium cation with alkyl chains of C_nH_{2n+1}; n = 4, 6, 8, 10, 12, 14, 16 and 18 for those with X = Br and I, and n = 12, 14, 16 and 18 for X = BF_4 and PF_6) under study are summarized in Fig. 1. The alkylation of vinylimidazole with corresponding alkyl halides afforded [C_nVIm]Br and [C_nVIm]I. While, [C_nVIm]BF_4 and [C_nVIm]PF_6 salts were prepared by anion metathesis of [C_nVIm]Br through treatment with sodium tetrafluoroborate or sodium hexafluorophosphate in methanol–water mixtures, respectively. Similarly, [C_{16}EIm]Br and [C_{16}EIm]I was prepared

Department of Chemistry, National Dong-Hwa University, Shoufeng, Hualien, 974, Taiwan. E-mail: ijblin@mail.ndhu.edu.tw; Fax: +886-3-863-3570; Tel: +886-3-863-3599

† Electronic supplementary information (ESI) available: Details of experimental preparation; characterization data for the salt synthesis; Table containing chemical shift and NMR spectrum. See DOI: 10.1039/c0jm02875d

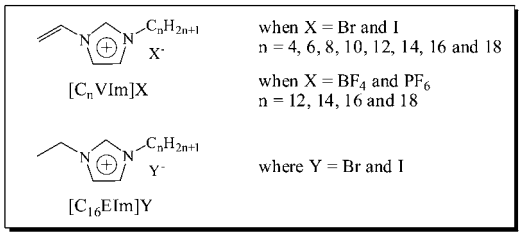

Fig. 1 General structure of salts studied.

by alkylation of ethylimidazole with 1-bromohexadecane or 1-iodohexadecane, respectively. All attempts to isolate a single crystal of vinylimidazolium salts, [C_nVIm]X, have been unsuccessful.

The liquid crystalline behavior of the vinylimidazolium salts were studied by differential scanning calorimetry (DSC), polarized optical microscopy (POM) and temperature controlled powder X-ray diffraction (PXRD) analysis. The transition temperatures and enthalpies of the vinylimidazolium salts are

Table 1 Phase behavior of 1-vinyl-3-alkylimidazolium salts, [C_nVIm]X[a,b]

Compound		Phase transition behavior
X = Br	$n = 18$[c]	Cr $\xrightarrow{70.5\ (93.4)}$ SmA $\xrightarrow{198}$ I[d]
	16	Cr $\underset{35.3(15.3)}{\overset{67.1(27.5)}{\rightleftharpoons}}$ SmA $\underset{157.2(0.3)}{\overset{157.6(0.3)}{\rightleftharpoons}}$ I
	14	Cr $\underset{32.9(21.6)}{\overset{59.8(35.7)}{\rightleftharpoons}}$ SmA $\underset{96.6(0.3)}{\overset{99.4(0.3)}{\rightleftharpoons}}$ I
	12	Cr $\underset{16.5(0.2)}{\overset{41.7(23.7)}{\rightleftharpoons}}$ I
X = I	$n = 18$	Cr $\underset{51.2(28.8)}{\overset{74.4(58.4)}{\rightleftharpoons}}$ SmA $\underset{185.3(0.5)}{\overset{186.4(0.5)}{\rightleftharpoons}}$ I
	16	Cr $\underset{33.7(22.5)}{\overset{40.9(9.0)}{\rightleftharpoons}}$ Cr′ $\underset{}{\overset{64.4(23.7)}{\rightarrow}}$ SmA $\underset{143.1(0.4)}{\overset{144.4(0.4)}{\rightleftharpoons}}$ I
	14	Cr $\underset{21.1(31.5)}{\overset{35.3(2.7)}{\rightleftharpoons}}$ Cr′ $\underset{}{\overset{60.9(43.2)}{\rightarrow}}$ SmA $\underset{90.4(0.4)}{\overset{90.9(0.4)}{\rightleftharpoons}}$ I
	12	Cr $\underset{19.52(0.2)}{\overset{34.5(0.6)}{\rightleftharpoons}}$ Cr′ $\underset{}{\overset{50.7(40.0)}{\rightarrow}}$ I
X = BF_4	$n = 18$	Cr $\underset{57.1(18.1)}{\overset{60.1(7.5)}{\rightleftharpoons}}$ Cr′ $\underset{}{\overset{65.1(25.1)}{\rightarrow}}$ SmA $\underset{156^{a}}{\overset{160.6(0.3)}{\rightarrow}}$ I
	16	Cr $\underset{44.4(38.5)}{\overset{48.4(5.9)}{\rightleftharpoons}}$ Cr′ $\underset{}{\overset{59.8(38.4)}{\rightarrow}}$ SmA $\underset{118.3(0.5)}{\overset{118.9(0.5)}{\rightleftharpoons}}$ I
	14	Cr $\underset{38.2(38.5)}{\overset{52.6(39.4)}{\rightleftharpoons}}$ SmA $\underset{61.1(0.3)}{\overset{61.6(0.3)}{\rightleftharpoons}}$ I
	12	Cr $\underset{< 0}{\overset{35.8(28.1)}{\rightleftharpoons}}$ I
X = PF_6	$n = 18$	Cr $\underset{81.2(55.4)}{\overset{91.0(60.0)}{\rightleftharpoons}}$ SmA $\underset{162.5(0.8)}{\overset{127.5(0.9)}{\rightleftharpoons}}$ I
	16	Cr $\underset{77.4(55.6)}{\overset{87.3(55.1)}{\rightleftharpoons}}$ SmA $\underset{89.1(0.7)}{\overset{89.7(0.7)}{\rightleftharpoons}}$ I
	14	Cr $\underset{69.5(32.3)}{\overset{79.3(32.8)}{\rightleftharpoons}}$ I
	12	Cr $\underset{54.6(28.8)}{\overset{68.5(28.9)}{\rightleftharpoons}}$ I

[a] Transition temperatures (°C) and enthalpies (kJ mol^{-1}, in parenthesis) are determined at a scan rate 2.0 °C min^{-1}. [b] Determined by POM as phase transition, since could not be observed under DSC. [c] Data from first heating cycle; Cr, Cr′ = crystal; SmA = smectic A; I = isotropic, I[d] = decomposition temperature.

Fig. 2 Representative POM image of $[C_{16}VIm]I$ at 100 °C.

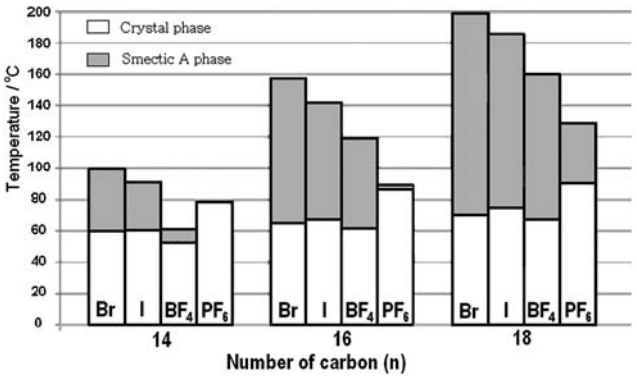

Fig. 3 Effect of chain length and anion on the mesogenic properties of vinylimidazolium salts, $[C_nVIm]X$ (n = 14, 16 and 18; and X = Br^-, I^-, BF_4^- and PF_6^-).

reported from the second heating cycle of the DSC studies and are provided in Table 1. On the second and subsequent heating and cooling cycles, the transitions are reproducible. However, in the case of $[C_{18}VIm]Br$ only the transition temperature from the first heating cycle is provided as decomposition occurs near the clearing point.

For the mesomorphic salts, $[C_{16}EIm]Br$, $[C_{16}EIm]I$, and $[C_nVIm]X$ (X = Br^-, I^- and BF_4^-; n = 14, 16 and 18, and X = PF_6^-; n = 16 and 18) a single enantiotropic mesophase with fan texture is observed by POM. We propose that the mesophase is a smectic A (SmA, Fig. 2) phase as is generally true for most of other *N*-alkyl substituted imidazolium based ILCs.[50–59] Samples cooled from the isotropic melt appear black (*i.e.* with uniform homeotropic domains) when they are viewed under a cross polarizer, which requires that the lamellar phases be uniaxial. On deformation/shearing, samples display an oily streaked texture resulted in transient focal conic domains, characteristic of SmA phase. This identification is supported by the PXRD data described later.

The effect of chain length and counter anion on the mesogenic properties of vinylimidazolium salts will be discussed first. In the Br^- series, compounds with n = 4, 6, 8 and 10 are room temperature ILs, and $[C_{12}VIm]Br$ is an IL above 41.7 °C. It is observed that as the alkyl chain length increases, the fluidity of the ILs decreases. The higher alkyl chain analogues, namely, $[C_{14}VIm]Br$, $[C_{16}VIm]Br$, and $[C_{18}VIm]Br$ are ILCs. DSC thermograms show that these salts have relatively low melting temperatures of transition from solid to mesophase: 59.8 °C for $[C_{14}VIm]Br$, 67.1 °C for $[C_{16}VIm]Br$, and 70.5 °C for $[C_{18}VIm]Br$. The clearing temperature increases rapidly with chain length: 99.4 °C for $[C_{14}VIm]Br$, 157.6 °C for $[C_{16}VIm]Br$, and up to 198 °C with decomposition for $[C_{18}VIm]Br$. $[C_{18}VIm]Br$ exhibits mesophase over a range of ΔT = 120 °C. In the I^- series, compounds with n = 4, 6, 8 and 10 are room temperature ILs and $[C_{12}VIm]I$ is an IL above 50.7 °C. Like the Br^- series, as the alkyl chain length increases fluidity of the ILs decreases. SmA phase is shown by $[C_{14}VIm]I$ from 60.9 to 90.9 °C, $[C_{16}VIm]I$ from 64.4 to 144.4 °C, and $[C_{18}VIm]I$ from 74.4 to 186.4 °C. Except for $[C_{16}VIm]I$, the melting temperatures are higher and the clearing temperatures are lower than those of the corresponding Br^- salts.

In the BF_4^- series, $[C_{12}VIm]BF_4$ is an ionic liquid above 35.8 °C, while the salts with n = 14, 16, and 18 exhibits LC phase, from 52.6 to 61.6 °C, 59.8 to 118.9 °C, and 65.1 to 160.6 °C, respectively. While in the case of PF_6^- series, $[C_{12}VIm]PF_6$ and $[C_{14}VIm]PF_6$ are ILs above 68.5 and 79.3 °C, respectively. The LC phase is seen for $[C_{16}VIm]PF_6$ from 87.3 to 89.7 °C and for $[C_{18}VIm]PF_6$ from 91.0 to 127.5 °C. The mesophase ranges are narrow, ΔT = 2 °C for $[C_{16}VIm]PF_6$ and 35 °C for $[C_{18}VIm]PF_6$. The lower homologues (n = 12 and 14), are ionic liquids above 55 °C. A severe supercooling phenomenon is observed in the crystallization, but is lesser in the isotropic to LC transition. Such a supercooling tendency has also been seen in other ILCs.[57–59]

Fig. 3 summarizes the phase transitions of the mesogenic vinylimidazolium salts among all the series. Formation of the mesomorphism depends on the type of anions and length of alkyl chains. There is a clear increase in both the melting and clearing points with an increase in the chain length (n) in each series. The mesophase range (ΔT) of any series increases by *ca.* 35 °C on increasing the alkyl chain length by two carbon atoms. The increase in the alkyl chain gives an increase in the temperature of clearing more than that of melting, showing a greater effect of the van der Waals interactions on the clearing temperature than on the melting temperature.[63]

Among the series of different anions, the trend in the melting point is roughly $BF_4^- \approx Br^- \approx I^- < PF_6^-$. In general, imidazolium salts with halide anions show higher melting temperatures than those with anions of PF_6^-, BF_4^- and ClO_4^-. However, PF_6^- salts showing higher melting temperatures are occasionally found.[51,64,65] In this work, a better packing of the PF_6^- anion in the vinyl imidazolium salts than the halide leads to a higher melting point for the former, whereas the clearing point and mesophase range follow the trend $PF_6^- < BF_4^- < I^- < Br^-$.[45,50] With an identical chain length, the process of transition from mesophase to isotropic liquid depends on the strength of cation–anion interactions, of which Coulombic and hydrogen bonding interactions are the two major interactions, the former interaction depends on the cation–anion size. With an identical cation, a smaller anion has a stronger Coulombic interaction. For the latter, the ^1H chemical shift of the carbenic C^2 proton is very sensitive to the anion present, and is a good indication of the strength of C^2-H···anion interaction. The stronger the hydrogen binding interaction, the lower the ^1H chemical shift of the carbenic proton. For example, for the $[C_{16}VIm]^+$ cation, the C^2 proton chemical shifts for different anions are δ 10.87 ppm for Br^-, δ 10.56 ppm for I^-, δ 9.14 ppm for BF_4^- and δ 8.86 ppm in

Table 2 Interlayer spacing of the vinylimidazolium and ethylimidazolium salts in Cr, and SmA phases

	d/Å (*T*/°C)			*d*/Å (*T*/°C)	
Salt	Cr	SmA	Salt	Cr	SmA
$[C_{18}VIm]Br$	64.4 (25)	37.8 (90)	$[C_{18}VIm]I$	18.5 (25)	37.4 (90)
$[C_{16}VIm]Br$	60.2 (25)	36.9 (90)	$[C_{16}VIm]I$	17.2 (25)	34.6 (90)
$[C_{14}VIm]Br$	56.0 (25)	31.8 (90)	$[C_{14}VIm]I$	15.9 (25)	31.4 (90)
$[C_{12}VIm]Br$	50.3 (25)	—	$[C_{12}VIm]I$	14.5 (25)	—
$[C_{16}EIm]Br$	31.6 (25)	35.3 (60)	$[C_{16}EIm]I$	29.9 (25)	34.1 (60)
$[C_{18}VIm]BF_4$	29.8 (25)	36.5 (90)	$[C_{18}VIm]PF_6$	30.8 (25)	35.7 (85)
$[C_{16}VIm]BF_4$	27.7 (25)	33.6 (90)	$[C_{16}VIm]PF_6$	28.9 (25)	33.8 (85)
$[C_{14}VIm]BF_4$	24.9 (25)	31.6 (60)	$[C_{14}VIm]PF_6$	26.5 (25)	—
$[C_{12}VIm]BF_4$	22.9 (25)	—	$[C_{12}VIm]PF_6$	24.2 (25)	—

the case of PF_6^-. Thus the order of the strength of three C–H···X hydrogen bonds is parallel to that of the Coulombic interaction.

To confirm the mesophase behavior and to understand the molecular arrangement of vinylimidazolium salts in the Cr and mesophase, PXRD are studied for the Br^-, I^-, BF_4^- and PF_6^- series salts as a function of temperature. All the salts displayed layered structures in both the crystal and liquid crystalline phases, in which the corresponding layer spacings are determined from the (001) reflections, and are in Table 2. The Cr phase *d* spacings of the vinylimidazolium salts in all series show a linear increment with chain length (*n*), indicating a similar structure for all the salts in the series (see the ESI, Fig. S1†).

Among the Br^-, I^-, BF_4^- and PF_6^- series, the PF_6^- series salts have the simplest PXRD results, so we will begin our discussion with this series, followed by the Br^-, I^-, and BF_4^- series. Fig. 4 represents diffractograms for the $[C_{18}VIm]PF_6$ at Cr and LC phase. The crystal phase shows that a set of equal spacing peaks at low angle region are observed suggesting a layer type structure with a corresponding layer spacing of 30.8 Å. For the lower homologue $[C_{16}VIm]PF_6$, a similar pattern with a layer spacing *d* of 28.9 Å is observed. Since the crystal layer spacing is $l < d < 2l$,

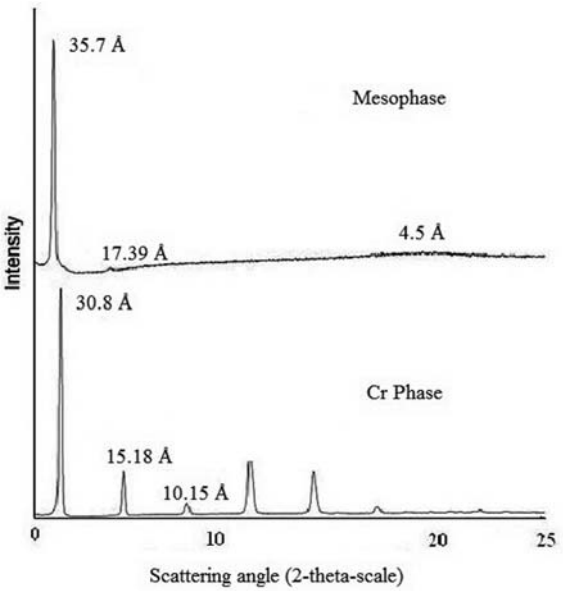

Fig. 4 PXRD pattern for $[C_{18}VIm]PF_6$ at Cr phase and at SmA phase.

where 'l' is the all-*trans* chain length, we propose that for the PF_6^- series compounds the crystal has an interdigitated bilayer structure. In the mesophase, there is a sharp (001) reflection followed by a weak (002) peak in the low angle region, and a faint diffused scattering at higher angles, suggesting a lamellar structure with a liquid like order of the alkyl chains in the layers. The wide angle peaks observed in the Cr phase are absent here, indicating a decrease in the positional ordering. There is an increment of 4.9 Å from Cr to mesophase for $[C_{18}VIm]PF_6$ and $[C_{16}VIm]PF_6$, which can be attributed to a decrease in the tilting angle of the molecular rod with respect to the plane normal. PXRD studies also show that the mesophase *d* spacing decreases steadily with increasing temperature (Fig. 5). This decrease is

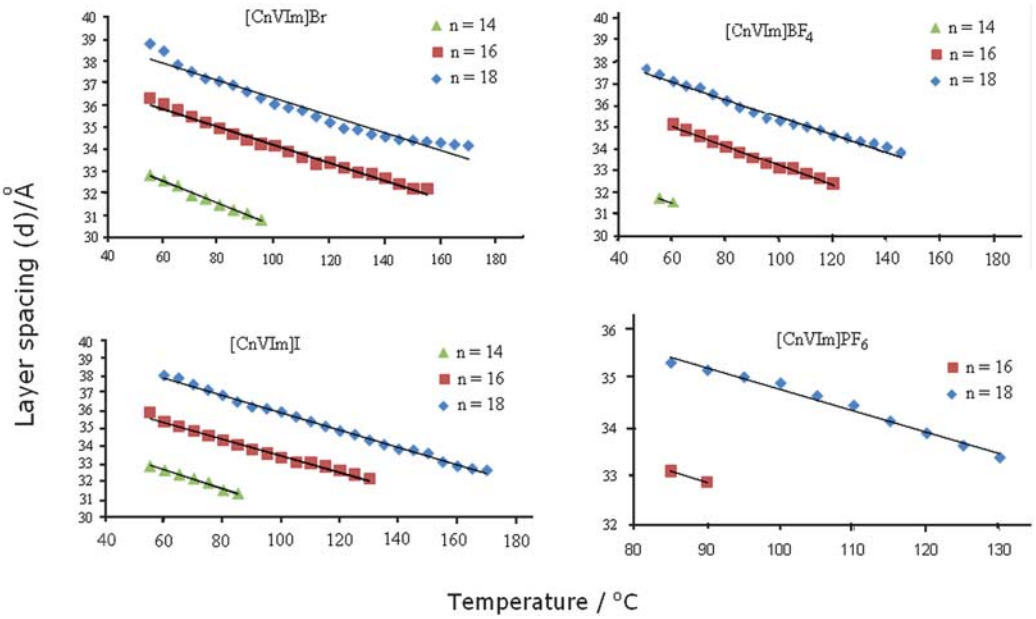

Fig. 5 Dependence of layer spacing *d* on temperature.

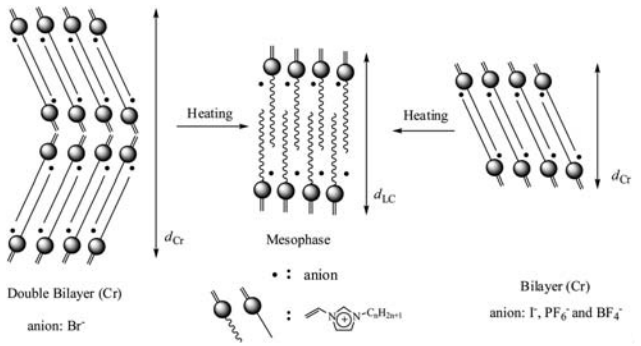

Fig. 6 Schematic representation of molecular arrangement in the Cr and SmA phases for $[C_nVIm]X$.

Table 3 Phase behavior of $[C_{16}EIm]X$.[a]

X	Phase transition behavior
Br	$Cr \underset{41.5(21.4)}{\overset{55.7(29.8)}{\rightleftharpoons}} SmA \underset{116.8(0.4)}{\overset{117.3(0.4)}{\rightleftharpoons}} I$
I	$Cr \underset{38.0(24.2)}{\overset{60.0(37.7)}{\rightleftharpoons}} SmA \underset{97.5(0.5)}{\overset{99.6(0.5)}{\rightleftharpoons}} I$

[a] Transition temperatures (°C) and enthalpies (kJ mol^{-1}, in parenthesis) are determined at a scan rate 2.0 °C min^{-1}; Cr = crystal phase; SmA = smectic A phase; I = isotropic phase.

attributed to a greater alkyl chain mobility upon increasing the temperature, and is consistent with an SmA phase as proposed.[66] A schematic diagram for the structure of the Cr and SmA phases are represented in Fig. 6.

The results are different for the salts of Br^- series. While the mesophase *d* spacing is similar to those for PF_6^- series, the Cr phase *d* spacing is almost double: 64.4 Å for $[C_{18}VIm]Br$, 60.2 Å for $[C_{16}VIm]Br$, and 56.0 Å for $[C_{14}VIm]Br$. We propose that the crystal either adopts a double bilayer structure, with alternating bilayers of different molecular conformations, or an extended bilayer structure, where the alkyl chains are not interdigitated. Since the layer spacing of 60.2 Å for $[C_{16}VIm]Br$ is more than double the molecular length of 25 Å,[67] the possibility to adopt the latter structure is unlikely. Hence we propose a double bilayer structure (Fig. 6), which has been observed for the 1-alkyl-3-methylimidazolium chloride salts.[68,69] In that example, two different conformations of the imidazolium ring heads with respect to the alkyl chains are found; one with chains more or less parallel to the ring (linear form), the other with chains almost perpendicular to the ring plane (bent form). After annealing, the salt exhibits only the most stable conformation (linear form). However, unlike in the report, the double bilayer structure changes to a simple bilayer structure, it thus reduces the *d* spacing. Similar to the PF_6^-series salts, the mesophase *d* spacing decreases steadily upon heating, confirming that the mesophase is the SmA phase Fig. 5.

The salts in the iodide series, $[C_nVIm]I$, have a *d* spacing of 14 to 19 Å, about one fourth of those for the Br^- and two thirds of the PF_6^- analogues in the Cr phase. It is possible that a bent conformation, which tilts with some angle from the normal of the layer plane, is adopted to give the short layer spacing. The mesophase structure for the iodide salts is similar to those of the other series of compounds, and has *d* spacings in the range of 31 to 37 Å, longer than those in the Cr phase but is comparable to those of the other series at the mesophase. PXRD studies shows that the mesophase *d* spacing decreases on increasing the temperature, again consistent with a SmA phase (Fig. 5). The plots in Fig. 5 are quasi-linear, the slight deviation of the plot from linearity in the mesophase has been observed in many cases.[26,70]

The mesogenic salts in the $[C_nVIm]BF_4$ series show *d* spacings between 24.9 and 29.8 Å in the Cr phase, which are comparable to those of the corresponding PF_6^- series. Therefore a simple bilayer structure is proposed for the crystal of the BF_4^- salts. The *d* spacing increases (*ca.* >21–27%) on transforming into the mesophase, similar to that observed for the PF_6^- series salts. The mesophase *d* spacing also decreases on increasing the temperature, typical for the SmA phase.

Despite the differences in the solid state structure, all the vinyl-substituted compounds have a similar structure at the mesophase between the different anions, the *d* spacing follows the order $Br^- > I^- > BF_4^- > PF_6^-$, a trend parallel to the size of the anions. The smaller anions could keep the cations closer, and confine the thermal movement of the alkyl chains to a stretched all-*trans* position. The larger anions keep the cations apart, allowing the chains to wriggle around.

To elucidate the unique properties of the *N*-vinyl substituent, ethyl substituted $[C_{16}EIm]Br$ and $[C_{16}EIm]I$ salts were utilized to compare the differences between the vinyl and saturated congeners in terms of structures, thermal behaviors, and cation–anion interactions. Table 3 provides the phase transition behavior of the ethylimidazolium salts. The ethylimidazolium salts exhibit liquid crystalline behavior of SmA based on POM and PXRD observations. $[C_{16}EIm]Br$ and $[C_{16}EIm]I$ have melting points of 55.7 and 60 °C, and clearing points of 117.3 and 99.6 °C, respectively. These values are compared to the vinyl analogues of $[C_{16}VIm]Br$ and $[C_{16}VIm]I$; melting points are 67.1 and 64.4 °C, and clearing points 157.6 and 144.4 °C, respectively. The vinyl compounds have a slightly higher melting point and substantially higher clearing point than their corresponding ethyl substituted compounds, and therefore a wider mesophase range; The ΔT = 61.6 °C for $[C_{16}EIm]Br$ and ΔT = 39.6 °C for $[C_{16}EIm]I$ are compared to the ΔT = 90.5 °C for $[C_{16}VIm]Br$ and ΔT = 80.0 °C for $[C_{16}VIm]I$ (see Table 1 and 3). The wider mesophase range observed for the vinylimidazolium salt is primarily due to the greater number of hydrogen bonding interactions between cations and anions, as will be discussed later.

At the Cr phase, $[C_{16}EIm]Br$ has a much smaller *d* spacing (31.6 Å) than that of the $[C_{16}VIm]Br$ (60.2 Å), whereas $[C_{16}EIm]I$ has a much larger *d* spacing (29.9 Å) than that of the $[C_{16}VIm]I$ (17.2 Å). A simple bilayer structure as for the BF_4^- and PF_6^- salts is adopted for these two ethyl substituted salts. At the mesophase, the two ethylimidazolium salts have a comparable layer structure to those of the vinyl analogue and hence a similar mesomorphic structure. Thus the presence of *N*-vinyl substituents leads to the formation of an unusual structure for the Br^- and I^- salts in the solid state, but not in the mesophase.

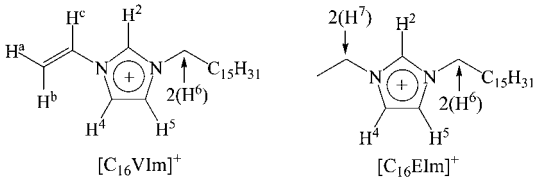

Fig. 7 Numbering of cationic proton of $[C_{16}VIm]^+$ and $[C_{16}EIm]^+$ under study.

Interaction of electron poor olefins with Br^- and I^- has been reported.[71–74] The positive charge of the imidazolium moiety could possibly promote the interaction of this *N*-vinyl substituent with halides, and thus gives arise to the unique crystal packing of the halide salts.

Recently the use of ^1H NMR technique to investigate the preferential site of interaction and the conformational behaviors of azolium-linked cyclophanes in the presence of increasing halide ion concentration in solution has been reported.[75,76] In this work similar experiments were employed to study the interaction of halide with $[C_{16}VIm]^+$ and $[C_{16}EIm]^+$. Tetrabutylammonium bromide (TBAB)/tetrabutylammonium iodide (TBAI) as a source of halide was added by portions to the $[C_{16}VIm]PF_6$ and $[C_{16}EIm]PF_6$ salts individually and monitored by ^1H NMR spectroscopy in CD_2Cl_2. To better describe the results, the numbering of the protons for the cations of $[C_{16}VIm]PF_6$ and $[C_{16}EIm]PF_6$ are shown in Fig. 7.

Results of the ^1H NMR spectra at the downfield region for the TBAB addition are given in Fig. 8, and the corresponding δ values for the TBAB addition are provided in the Table 4. Those of the TBAI addition are provided in the ESI.† The chemical shift of the carbenic H^2 of $[C_{16}VIm]PF_6$ appears at δ 8.86 ppm and the corresponding signal for the $[C_{16}VIm]Br$ appears further downfield at δ 10.87 ppm. Addition of one equivalent of TBAB to $[C_{16}VIm]PF_6$ in CD_2Cl_2 results in downfield shifting of the H^2 from δ 8.86 to 10.43 ppm ($\Delta\delta$ = 1.57 ppm). This change in the chemical shift of the H^2 is due to its interaction with the bromide ion in solution. Likewise the imidazolium H^4 and H^5 are observed slightly downfield from δ = 7.33 to 7.43 ppm ($\Delta\delta$ = 0.10 ppm) and from δ = 7.53 to 7.71 ppm ($\Delta\delta$ = 0.18 ppm), respectively, suggesting that in addition to the H^2, bromide ion also has influences on the imidazolium H^4 and H^5, but to a much smaller extent. For the vinylic H^c next to the imidazolium *N* atom, a slightly larger change from 7.03 to 7.37 ppm in the chemical shifts is found (Fig. 8). The vinylic H^b also shows a downfield shift from δ = 5.79 to 5.93 ppm while H^a behaves differently and appears upfield at δ = 5.42 ppm. Addition of two and three equivalents of TBAB to the $[C_{16}VIm]PF_6$ solution results in further downshift of the H^2 proton to δ = 10.85 ppm then to δ = 10.95 ppm; the changes are, however, smaller compared to that of the addition of the first equivalent of TBAB. Furthermore, there is very little effect on the other head group protons with additional TBAB (Fig. 8). Experiments carried out with 1–3 equivalents of TABI give results similar to yet have smaller influences than that carried out with TBAB (see ESI Fig. S2 and Table S1†).

For the corresponding ethylimidazolium compound $[C_{16}EIm]PF_6$, the chemical shift for the carbenic H^2 appears at δ 8.89 ppm and the corresponding signal for the $[C_{16}EIm]Br$ appears much downfield at δ 10.34 ppm. Addition of one equivalent of TBAB to $[C_{16}EIm]PF_6$ in CD_2Cl_2 results in

Table 4 NMR peak values for the $[C_{16}VIm]PF_6$ and $[C_{16}EIm]PF_6$ protons

			Chemical shift for the corresponding proton in CD_2Cl_2, δ/ppm							
Compound	Additive	Ratio	H^2	H^4	H^5	H^7	H^6	H^a	H^b	H^c
$[C_{16}VIm]PF_6$	None	—	8.77	7.37	7.56	—	4.21	5.48	5.79	7.08
$[C_{16}VIm]PF_6$	TBAB	1 : 1	10.43	7.43	7.71	—	4.31	5.40	5.93	7.37
$[C_{16}VIm]PF_6$	TBAB	1 : 2	10.85	7.53	7.89	—	4.33	5.36	6.15	7.46
$[C_{16}VIm]PF_6$	TBAB	1 : 3	10.95	7.60	8.01	—	4.33	5.33	6.08	7.50
$[C_{16}EIm]PF_6$	None	—	8.89	7.32	7.28	4.30	4.20	—	—	—
$[C_{16}EIm]PF_6$	TBAB	1 : 1	10.06	7.41	7.33	4.35	4.26	—	—	—
$[C_{16}EIm]PF_6$	TBAB	1 : 2	10.32	7.50	7.38	4.37	4.28	—	—	—
$[C_{16}EIm]PF_6$	TBAB	1 : 3	10.41	7.57	7.43	4.37	4.28	—	—	—

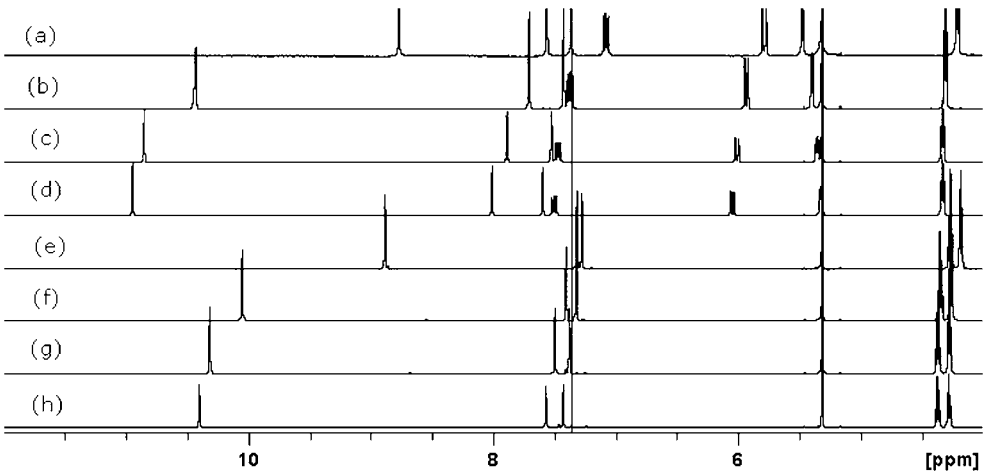

Fig. 8 Downfield region of the ^1H NMR spectra (600 MHz) in CD_2Cl_2 of (a) $[C_{16}VIm]PF_6$, (b) $[C_{16}VIm]PF_6$ + TBAB (1 : 1), (c) $[C_{16}VIm]PF_6$ + TBAB (1 : 2), (d) $[C_{16}VIm]PF_6$ + TBAB (1 : 3), (e) $[C_{16}EIm]PF_6$, (f) $[C_{16}EIm]PF_6$ + TBAB (1 : 1), (g) $[C_{16}EIm]PF_6$ + TBAB (1 : 2), (h) $[C_{16}EIm]PF_6$ + TBAB (1 : 3).

a downfield shifting of H^2 from δ 8.89 to 10.06 ppm ($\Delta\delta$ = 1.17 ppm). Likewise the chemical sifts of the signals for the imidazolium H^4 and H^5 protons are observed slightly downfield (Table 4). *N*-Alkyl protons of H^6 and H^7, unlike the *N*-vinylic H^c proton, show very little change in the chemical shift (*ca.* $\delta = 0.05$ ppm) in the presence of Br^-. Utilizing TBAI instead of TBAB results in a similar observation (see ESI Fig. S2 and Table S1†).

The halide addition studies described above suggest that the negatively charged anion attempts to locate at the vicinity of the imidazolium cation. Since the chemical shift of the imidazolium H^2 is the most influenced, the interaction between the halide and the carbenic proton is the strongest one. The vinylic H^c is the next higher to be influenced. That is, the presence of *N*-vinyl group provides additional and favorable bonding sites for C–H···X interactions. It can be concluded that more hydrogen bonding interaction between the imidazolium cations and anions stabilizes the mesophase to a large extent.

Conclusions

In this work, ionic liquids and ionic liquid crystals based on 1-vinyl-3-alkylimidazolium salt, [C_nVIm]X, were prepared and characterized. Salts with $n \leq 12$ are RTILs and those with longer alkyl chains exhibit an SmA phase. In the solid state, the bromide salts in the vinylimidazolium series exhibit a double bilayer structure, whereas all the other vinyl and ethyl substituted salts adopt a simple bilayer structure. Although the exact nature is not certain, the special interaction between the vinyl group and halide in the solid causes diverse structures in the vinyl imidazolium salts. In the mesophase, all the compounds have a similar bilayer structure.

The mesophase range increases with an increase in the alkyl chain length and decreases with anion size $Br^- > I^- > BF_4^- > PF_6^-$. A comparison of the mesophase range between the pairs of [C_{16}VIm]Br/[C_{16}EIm]Br and [C_{16}VIm]I/[C_{16}EIm]I, clearly indicates that the presence of vinyl substituent substantially enhances the mesophase range over that of the ethyl substituted congeners. Results from ^{1}H NMR studies suggest that the chemical shift of the carbenic proton depends on the anion and is an indication of the strength of the C–H···X hydrogen bonding interaction, where X follows the order: $Br^- > I^- > BF_4^- > PF_6^-$. Results also show that the *N*-vinyl substituent provides an additional strong C–H···X hydrogen bonding interaction, in which the strength decreases with increasing anion size.

Experimental

General experimental procedures for one salt each from vinylimidazolium series are provided here and detailed experimental procedures with characterization of all other salts are provided in the ESI.†

Synthesis of 1-vinyl-3-octadecylimidazolium bromide, [C_{18}VIm]Br·H_2O

1-Vinyl-3-octadecylimidazolium bromide salt has been prepared from the *N*-alkylation of 1-vinylimidazole (1 eq.) with the 1-bromooctadecene (1 eq.). Under dry nitrogen atmosphere and vigorous stirring, freshly distilled 1-bromooctadecene was added drop-wise over a period of 2 h to the reaction mixture. After the addition is complete the reaction mixture was kept refluxing for about 3 h till consumption of vinylimidazole, as indicated by TLC. The crude product was washed with diethyl ether to remove unreacted starting materials, if any. Furthermore, the crude product was recrystallized from DCM/ether to give a light yellow solid with a yield >98%. ^{1}H NMR (ppm, $CDCl_3$): δ 0.86 (t, $J^3 = 6.3$ Hz, 3H, CH_3), 1.04–1.32 (m, 30H, CH_2), 1.84–2.00 (m, 2H, CH_2), 4.39 (t, $J^3 = 7.38$, 2H, CH_2), 5.38–5.98 (m, 2H, CH_2), 7.44 (s, 1H, CH), 7.46–7.53 (q, H, CH), 7.74 (s, 1H, CH), 10.98 (s, 1H, CH). Anal. calculated for $C_{23}H_{45}N_2OBr$: C, 62.01; H, 10.18; N, 6.29. Found: C, 62.13; H, 10.21; N, 6.19.

Synthesis of 1-vinyl-3-octadecylimidazolium iodide, [C_{18}VIm]I

1-Vinyl-3-octadecylimidazolium Iodide was prepared from the *N*-alkylation of 1-vinylimidazole (1 eq.) with 1-iodooctadecene (1 eq.). Under dry nitrogen atmosphere and vigorous stirring, freshly distilled 1-bromooctadecene was added drop-wise over a period of 2 h to reaction mixture. After the addition is complete the reaction mixture was kept refluxing for about 3 h till consumption of vinylimidazole, as indicated by TLC. The crude product was washed with diethyl ether to remove unreacted starting materials, if any. Furthermore, the crude product was recrystallized from DCM/ether to give a light yellow solid with a yield >99%. ^{1}H NMR (ppm, $CDCl_3$): δ 0.85 (t, $J^3 = 6.3$ Hz, 3H, CH_3), 1.22–1.32 (m, 30H, CH_2), 1.89–1.96 (m, 2H, CH_2), 4.40 (t, $J^3 = 7.38$, 2H, CH_2), 5.39–6.02 (m, 2H, CH_2), 7.56 (s, 1H, CH), 7.37–7.46 (q, H, CH), 7.83 (s, 1H, CH), 10.51 (s, 1H, CH). Anal. calculated for $C_{23}H_{43}N_2I$: C, 62.01; H, 10.18; N, 6.29. Found: C, 62.13; H, 10.21; N, 6.19.

Synthesis of 1-vinyl-3-octadecylimidazolium tetrafluoroborate, [C_{18}VIm]BF_4

[C_{18}VIm]BF_4 was prepared by anion metathesis of [C_{18}VIm]Br·H_2O salts, in MeOH–H_2O (20 : 80 v/v) solvent system using NH_4BF_4. The precipitates were isolated by filtration. The crude product obtained was washed with a lot of MeOH–H_2O (20 : 80 v/v). A colorless solid was obtained with 70% yield. ^{1}H NMR (ppm, $CDCl_3$): $\delta = 0.87$ (t, $J^3 = 6.4$ Hz, 3H, CH3), 1.25–1.37 (m, 30H, CH_2), 1.89–1.91 (m, 2H, CH_2), 4.24 (t, $J^3 = 7.3$ Hz, 2H, CH_2), 5.37–5.84 (m, 2H, CH_2), 7.10–7.19 (q, H, CH), 7.40 (s, 1H, CH), 7.63 (s, 1H, CH), 9.12 (s, 1H, CH). Anal. calculated for $C_{23}H_{43}N_2BF_4$: C, 63.59; H, 6.45; N, 9.87. Found: C, 63.20; H, 6.03; N, 9.78.

Synthesis of 1-vinyl-3-octadecylimidazolium hexafluorophosphate, [C_{18}VIm]PF_6

[C_{18}VIm]PF_6 was prepared by anion metathesis of [C_{18}VIm]Br·H_2O salts, MeOH–H_2O (15 : 85 v/v) solvent system using NH_4PF_6. The precipitates were isolated by filtration. The crude product obtained was washed with a lot of MeOH–H_2O (15 : 85 v/v). A colorless solid product was obtained with about 70% yield. ^{1}H NMR (ppm, $CDCl_3$): δ 0.88 (t, $J^3 = 6.3$ Hz, 3H, CH_3), 1.25–1.33 (m, 30H, CH_2), 1.87–1.92 (m, 2H, CH_2), 4.21 (t, $J^3 = 7.38$, 2H, CH_2), 5.40–5.80 (m, 2H, CH_2), 7.03–7.11 (q, H, CH), 7.33 (s, 1H, CH), 7.54 (s, 1H, CH), 8.84 (s, 1H, CH). Anal. calculated for $C_{23}H_{43}N_2PF_6$: C, 50.00; H, 8.15; N, 7.23. Found: C, 52.64; H, 7.63; N, 7.23.

Acknowledgements

We thank the National Science Council of Taiwan (Grant no. NSC 97-2113-M-259-009-MY3) for the financial support of this work.

References

1 T. Welton, *Chem. Rev.*, 1999, **99**, 2071, and references therein.
2 A. B. McEwen, H. L. Ngo, K. LeCompte and J. L. Goldman, *J. Electrochem. Soc.*, 1999, **146**, 1687.
3 R. Sheldon, *Chem. Commun.*, 2001, 2399.
4 P. Wasserscheid and W. KEIm, *Angew. Chem., Int. Ed.*, 2000, **39**, 3772.
5 J. Dupont, P. A. Z. Suarez, A. P. Umpierre and R. F. Souza, *J. Braz. Chem. Soc.*, 2000, **11**, 293.
6 J. Ding and D. W. Armstrong, *Chirality*, 2005, **17**, 281.
7 K. M. Docherty, J. K. Dixon and C. F. Kulpa Jr, *Biodegradation*, 2007, **18**, 481.
8 P. Wasserschied, T. Welton, *Ionic Liquids in Synthesis*; Wiley-VCH, WeinhEIm, 2003, and references therein.
9 J. S. Wilkes, *Green Chem.*, 2002, **4**, 73, and references therein.
10 H. Ohno, *Bull. Chem. Soc. Jpn.*, 2006, **79**, 1665–1680.
11 K. R. Seddon, *J. Chem. Technol. Biotechnol.*, 1997, **68**, 351.
12 C. M. Gordon, *Appl. Catal., A*, 2001, **222**, 101.
13 H. Olivier-Bourbigou and L. Magna, *J. Mol. Catal. A*, 2002, **182–183**, 419.
14 J. Dupont, R. F. de Souza and P. A. Z. Suarez, *Chem. Rev.*, 2002, **102**, 3667.
15 T. Welton, *Coord. Chem. Rev.*, 2004, **248**, 2459.
16 J. Dupont, R. D. F. Souza and P. A. Z. Suarez, *Chem. Rev.*, 2002, **102**, 3667.
17 Z. S. Wang, N. Koumura, Y. Cui, M. Miyashita, S. Mori and K. Hara, *Chem. Mater.*, 2009, **21**, 2810.
18 R. Kawano, H. Matsui, C. Matsuyama, A. Satoh, M. A. B. H. Susan, N. Tanabe and M. Watanebe, *J. Photochem. Photobiol., A*, 2004, **164**, 87.
19 S. M. Zakeeruddin and M. Gratzel, *Adv. Funct. Mater.*, 2009, **19**, 2187.
20 Y. Zhou, *Curr. Nanosci.*, 2005, **1**, 35.
21 C. N. R. Rao, S. R. C. Vivekchand, Kanishka Biswas and A. Govindaraj, *Dalton Trans.*, 2007, 3728.
22 R. J. Soukup-Hein, M. M. Warnke and D. W. Armstrong, *Annu. Rev. Anal. Chem.*, 2009, **2**, 145.
23 M. D. Green and T. E. Long, *Polym. Rev.*, 2009, **49**, 291.
24 W. Dobbs, J.-M. Suisse, L. Douce and R. Welter, *Angew. Chem., Int. Ed.*, 2006, **45**, 4179.
25 J.-M. Suisse, L. Douce, S. Bellemin-Laponnaz, A. Maisse-François, R. Welter, Y. Miyake and Y. Shimizu, *Eur. J. Inorg. Chem.*, 2007, 3899.
26 W. Dobbs, B. Heinrich, C. Bourgogne, B. Donnio, E. Terazzi, M.-E. Bonnet, F. Stock, P. Erbacher, A.-L. Bolcato-Bellemin and L. Douce, *J. Am. Chem. Soc.*, 2009, **131**, 13338.
27 J. C. Salamone, S. C. Israel, P. Taylor and B. Snider, *Polymer*, 1973, **14**, 639.
28 M. Yoshizawa, M. Hirao, K. Ito-Akita and H. Ohno, *J. Mater. Chem.*, 2001, **11**, 1057.
29 G. H. Min, T. Yim, H. Y. Lee, D. H. Huh, E. Lee, J. Mun, S. M. Oh and Y. G. Kim, *Bull. Korean Chem. Soc.*, 2006, **27**, 847.
30 Y. N. Hsieh, R. S. Horng, W. Y. Ho, P. C. Huang, C. Y. Hsu, T. J. Whang and C. H. Kuei, *Chromatographia*, 2008, **67**, 413.
31 A. Orita, K. Kamijima and M. Yoshida, *J. Power Sources*, 2010, **195**, 7471.
32 F. Mazille, Z. Fei, D. Kuang, D. Zhao, S. M. Zakeeruddin, M. Gratzel and P. J. Dyson, *Inorg. Chem.*, 2006, **45**, 1585.
33 K. M. Son, M. G. Kang, R. Vittal, J. Lee and K. J. Kim, *J. Appl. Electrochem.*, 2008, **38**, 1647.
34 M. Yoshizawa, M. Hirao, K. I. Akita and H. Ohno, *J. Mater. Chem.*, 2001, **11**, 1057.
35 D. Batra, S. Seifert, L. M. Varela, A. C. Y. Liu and M. A. Firestone, *Adv. Funct. Mater.*, 2007, **17**, 1279.
36 S. Amajjahe and H. Ritter, *Macromolecules*, 2008, **41**, 716.
37 Y. N. Hsieh, R. S. Horng, W. Y. Ho, P. C. Huang, C. Y. Hsu, T. J. Whang and C. H. Kuei, *Chromatographia*, 2008, **67**, 413.
38 Z. Fei, T. J. Geldbach, D. Zhao and P. J. Dyson, *Chem.–Eur. J.*, 2006, **12**, 2122.
39 H. Yoshizawa, T. Mihara and N. Koide, *Liq. Cryst.*, 2005, **32**, 143.
40 X. D. Mu, J. Q. Meng, Z. C. Li and Y. Kou, *J. Am. Chem. Soc.*, 2005, **127**, 9694.
41 D. Wei, H. E. Unalan, D. Han, Q. Zhang, L. Niu, G. Amaratunga and T. Ryhanen, *Nanotechnology*, 2008, **19**, 1.
42 K. Binnemans, *Chem. Rev.*, 2007, **107**, 2592, and references therein.
43 N. Yamanaka, R. Kawanp, W. Kubo, T. Kitamura, Y. Wada, M. Watanabe and S. Yanagida, *Chem. Commun.*, 2005, 740.
44 J. Y. Z. Chiou, J. N. Chen, J. S. Lei and I. J. B. Lin, *J. Mater. Chem.*, 2006, **16**, 2972.
45 C. K. Lee, K. M. Lee and I. J. B. Lin, *Organometallics*, 2002, **21**, 10.
46 C. K. Lee, H. W. Huang and I. J. B. Lin, *Chem. Commun.*, 2000, 1911.
47 M. Yoshio, T. Ichikawa, H. Shimura, T. Kagata, A. Hamasaki, T. Mukai, H. Ohno and T. Kato, *Bull. Chem. Soc. Jpn.*, 2007, **80**, 1836.
48 M. Yoshio, T. Mukai, H. Ohno and T. Kato, *J. Am. Chem. Soc.*, 2004, **126**, 994.
49 M. Yoshio, T. Kagata, K. Hoshino, T. Mukai, H. Ohno and T. Kato, *J. Am. Chem. Soc.*, 2006, **128**, 5570.
50 B. K. Cho, A. Jain, S. M. Gruner and U. Wiesner, *Science*, 2004, **305**, 1598.
51 K. M. Lee, C. K Lee. and I. J. B. Lin, *Chem. Commun.*, 1997, 899.
52 D. Ster, U. Baumeister, C. J. Lorenzo, C. Tschierske and G. Israel, *J. Mater. Chem.*, 2007, **17**, 3393.
53 W. Dobbs, L. Douce, L. Allouche, A. Louati, F. Malbosc and R. Welter, *New J. Chem.*, 2006, **30**, 528.
54 M. Yoshio, T. Mukai, H. Ohno and T. Kato, *J. Am. Chem. Soc.*, 2004, **126**, 994.
55 M. Yoshio, T. Mukai, H. Ohno, and T. Kato, *ACS Symposium Series, Vol. 975 Ionic Liquids IV*, Chapter 11, pp. 161–171.
56 K. M. Lee, Y. T. Lee and I. J. B. Lin, *J. Mater. Chem.*, 2003, **13**, 1079.
57 K. M. Lee, J. C. C. Chen, C. J. Huang and Ivan J. B. Lin, *CrystEngComm*, 2009, **11**, 2804.
58 S. Lee, G. A. Becht, B. Lee, C. T. Burns and M. A. Firestone, *Adv. Funct. Mater.*, 2010, **20**, 1.
59 G. H. Min, T. Yim, H. Y. Lee, D. H. Huh, E. Lee, J. Mun, Seung M. Oh and Y. G. Kim, *Bull. Korean Chem. Soc.*, 2006, **27**, 847.
60 J. Wu, J. Zhang, H. Zhang, J. He, Q. Ren and M. Guo, *Biomacromolecules*, 2004, **5**, 266.
61 D. Batra, S. Seifert, L. M. Varela, A. C. Y. Liu and M. A. Firestone, *Adv. Funct. Mater.*, 2007, **17**, 1279.
62 S. Lee, M. D. Cummins, G. A. Willing and M. A. Firestone, *J. Mater. Chem.*, 2009, **19**, 8092.
63 M. Trilla, R. Pleixats, T. Parella, C. Blanc, P. Dieudonné, Y. Guari and M. W. C. Man, *Langmuir*, 2008, **24**, 259.
64 M. Veber, C. Jallabert, H. Strzelecka, V. Gionis and G. Sigaud, *Mol. Cryst. Liq. Cryst.*, 1986, **137**, 373.
65 P. H. J. Kouwer and T. M. Swager, *J. Am. Chem. Soc.*, 2007, **129**, 14042.
66 C. K. Lee, C. S. Vasam, T. W. Huang, H. M. J Wang, R. Y. Yang, C. S. Lee and I. J. B. Lin, *Organometallics*, 2006, **25**, 3768.
67 The approximate molecular length can be calculated using ChemDraw software.
68 A. E. Bradley, C. Hardacre, J. D. Holbrey, S. Johnston, S. E. J. McMath and M. Nieuwenhuyzen, *Chem. Mater.*, 2002, **14**, 629.
69 A. Downard, M. J. Earle, C. Hardacre, S. E. J. McMath, M. Nieuwenhuyzen and S. J. Teat, *Chem. Mater.*, 2004, **16**, 43.
70 W. Dobbs*, L. Douce and B. Heinrich, *Beilstein J. Org. Chem*, 2009, **5**(N0. 62), 1.
71 O. B. Berryman, F. Hof, M. J. Hynesc and D. W. Johnson, *Chem. Commun.*, 2006, 506.
72 H. Schneider, K. M. Vogelhuber, F. Schinle and J. M. Weber, *J. Am. Chem. Soc.*, 2007, **129**, 13022.
73 Y. S. Rosokha, S. V. Lindeman, S. V. Rosokha and J. K. Kochi, *Angew. Chem. Int. Ed.*, 2004, **116**, 4750.
74 B. L. Schottel, H. T. Chifotides and K. R. Dunbar, *Chem. Soc. Rev.*, 2008, **37**, 68.
75 M. V. Baker, M. J. Bosnich, D. H. Brown, L. T. Byrne, V. J. Hesler, B. W. Skelton, A. H. White and C. C. Williams, *J. Org. Chem.*, 2004, **69**, 7640.
76 M. V. Baker, D. H. Brown, C. H. Heath, B. W. Skelton, A. H. White and C. C. Williams, *J. Org. Chem.*, 2008, **73**, 9340.

